Energy Equip. Sys./ Vol. 8/No. 2/June 2020/ 103-110

ENERGY EQUIPSYS

Energy Equipment and Systems

http://energyequipsys.ut.ac.ir
www.energyequipsys.com

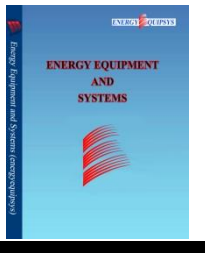

Solar cell efficiency enhancement using a hemisphere texture containing metal nanostructures

Authors

Mohammad Bashirpour [a]
Jafar Poursafar [a]
Mohammadreza Kolahdouz [a*]

[a] School of Electrical and Computer Engineering, University of Tehran, Tehran, Iran

Article history:

Received : 13 January 2019
Accepted : 18 January 2019

ABSTRACT

One major problem of the conventional solar cells is low conversion efficiency. In this work, we have proposed a new design including hemisphere texturing on top and metallic plasmonic nanostructure under the silicon layer to enhance the optical absorption inside the photosensitive layer. The finite-difference time-domain (FDTD) method has been used to investigate the interaction of light with the proposed structure. The simulation results demonstrated that the designed structure gives rise to 40% light absorption enhancement and 27% solar cell efficiency enhancement compared to a simple cell structure. The hemisphere texturing acts as a light concentrator and results in local electric field enhancement inside the silicon layer, and metallic nanostructure excites the plasmons. By combining the advantages of these two designs, the short circuit of the proposed structure showed more than 65% enhancement compared to the conventional structure.

Keywords: Hemisphere Surface, Plasmonic, Nanostructures, Silicon, Solar Cells.

1. Introduction

Two basic problems in silicon-based solar cells are the high cost of fabrication and low efficiency. Forty percent of the financial budget spends on the materials and processes carried out on them at the solar cell fabrication industry. Therefore, a reduction in the thickness of silicon causes a reduction in the cost of solar cells. Recently, thin-film solar cells with a very thin active layer have been proposed as a way to reduce the material costs. Beside low manufacturing costs, this reduction in the thickness of the solar cells can also decrease the carrier recombination rate and improve the carrier collection efficiency for bulk recombination-dominated semiconductors. As a result, we may have higher overall solar cell efficiencies. However, thin-film solar cells have a very low light absorption, especially at the wavelengths near the electronic bandgap of the semiconductor [1]–[3]. This is because of decreasing the light pathway through the active layer as a result of the reduction of absorber thickness. Therefore, some technics for light trapping are needed to design ultrathin solar cells with enhanced light absorption [4]–[7]. In the last few years, several techniques have been investigated for light trapping, such as forming pyramid shapes on the surface. The surface shaping generally reduces light reflection and thus increases its absorption.

* Corresponding author: Mohammadreza Kolahdouz
School of Electrical and Computer Engineering, University of Tehran, Tehran, Iran
Email: kolahdouz@ut.ac.ir

The other option for further absorption of the light in thin-layer solar cells is by adding nanoparticles and nanostructures to the solar cells structures [8]–[12]. In this work, we have introduced a new structure that benefits from both surface texturing and metallic plasmonic nanostructures to improve the light absorption in thin-film solar cells.

2. Structure design and simulation method

Finite-difference time-domain (FDTD) method is used to solve the Maxwell wave equations. The boundary conditions in the propagation direction were set to a perfectly matched layer (PML). The absorption of light in the mentioned thin-film solar cell can be defined as the ratio of the absorption capacity of the absorbent material to the power of the input light to the cell. In the simulation procedure, first, the optical response was calculated by solving Maxwell's equation [13], [14]:

$$\nabla \times \mu_r^{-1}(\nabla \times \vec{E}) - k_o^2(\varepsilon_r - \frac{j\lambda\sigma}{2\pi c\varepsilon_o})\vec{E} = 0 \quad (1)$$

After that, the electrical field distribution in each point of the simulation domain has been obtained by solving Eq. (1). Power flux density was calculated as followed:

$$P_{ox}(x,y,z) = \frac{1}{2\eta}\mathrm{Re}(|E_y|^2 - |E_z|^2) \quad (2)$$

$$P_{oy}(x,y,z) = \frac{1}{2\eta}\mathrm{Re}(|E_z|^2 - |E_x|^2) \quad (3)$$

$$P_{oz}(x,y,z) = \frac{1}{2\eta}\mathrm{Re}(|E_x|^2 - |E_y|^2) \quad (4)$$

In Eq. (2-4), η is material dependent complex wave impedance. The total power flux density can be obtained as followed:

$$P_s(x,y,z) = \left(|P_{ox}(x,y,z)|^2 + |P_{oy}(x,y,z)|^2 + |P_{oz}(x,y,z)|^2\right) \quad (5)$$

The main FDTD simulation parameters used in the simulations are presented in Table 1.

Figure 1a, b and c illustrate the schematic diagram of simple Si solar cell (Structure A), hemisphere textured cell without nano stripe (Structure B), and textured cell with a hemisphere and with the addition of aluminum nano stripe (structure c), respectively. As this figure shows, the hemisphere radius is 1 μm, and the thickness of the silicon layer is 600 nm. In other words, the whole thickness of the absorbent material (silicon) was considered to be 1.6 μm. The thickness of the antireflection layer is 200 nm.

The back contact of the cell, a cross made of aluminum nanostripes, can be seen in Fig. 1. The junction layer thickness is 400 nm, and the number of these nanostripes is four, with a 45-degree relative to each other. The width and thickness of these nanostripes were 180 nm and 90 nm, respectively.

3. Results and Discussion

In order to enhance the light absorption inside the Si layer, two different technics have been used. First, texturing the surface of the cell in the form of hemispheres and second, adding metallic nanostripes to the back contact of the cell. Therefore, we first examine the changes in the characteristics of the cell by forming its surface to a hemisphere. Here, we have used Snell's law for the hemisphere surfaces. That is,

$$x^2 = R^2 + r^2 - 2r\cos(\theta - \gamma), \quad (6)$$

$$\frac{x}{\sin(\theta-\gamma)} = \frac{r}{\sin\beta} \text{ and} \quad (7)$$

$$\frac{\sin\gamma}{\sin\beta} = n(\lambda). \quad (8)$$

In these equations, x is the length of the light path inside the cell, R is the hemisphere's radius, r(θ,γ) represents the coordinates of the

Table 1. Finite-Difference Time-Domain Method Parameters

Min mesh step (nm)	0.25
Time step d_t (fs)	0.075822
Stability factor	0.99
Simulation time (fs)	1000
Min sampling per cycle	2
frequency point	177

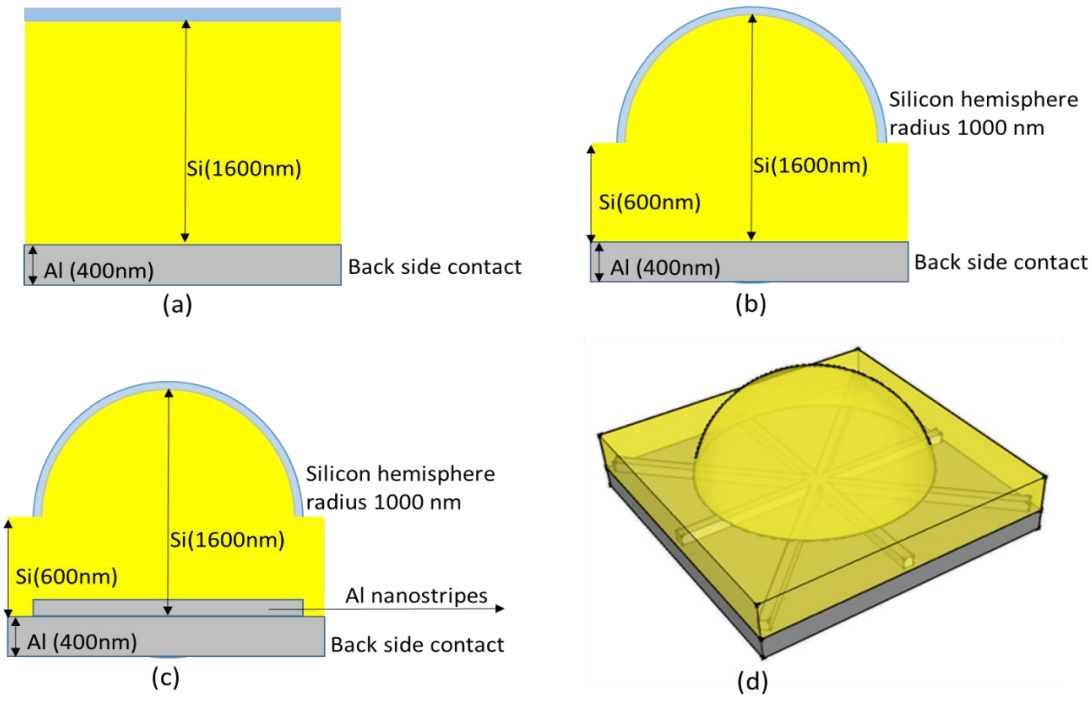

Fig. 1. Schematic diagram of a) simple Si solar cell (Structure A) b) Si solar cell with hemisphere texturing on top (Structure B) c) proposed Si solar cell with hemisphere texturing on top and metallic plasmonic nanostructure under the silicon layer Solar cell (Structure C) d) 3D view of proposed Si solar cell with hemisphere texturing on top and metallic plasmonic nanostructure under the silicon layer Solar cell.

desired point in the hemisphere, β is the angle of refraction, n(λ) symbolizes the refractive index and λ denotes the wavelength. It is determined that as a result of the non-flat feature of the surface, the angle of light refraction changes proportional to the position. Thus, at any point on the surface, the angle of the incoming light beam is different. For example, as shown in Fig. 2, if the light is vertically incident upon the center of the hemisphere, it has a 90-degree angle to the surface of the hemisphere. However, if it strikes the surface of the cell at a point a bit to the right (but still on the hemisphere), this angle decreases a little. Consequently, the refractive index of the light depends on its position on the hemisphere surface, and the light deflection occurs in the way that the light tends to the center of the hemisphere. In other words, the half-sphere acts like a lens and guides light to its center. Hence, the intensity of the light, and therefore, the intensity of the electric field raises at the center of the hemisphere [15]. Given that the absorption of light has an exponential relation with the intensity of the electric field (E^2 ~ Abs), the absorption of the light, and thus the carrier generation increases by approaching to the center of the hemisphere. Electric field distribution of Structure A, B and C at the X-Z plane are illustrated in Fig. 2a-c, respectively. As can be seen, using hemispheric texture on top of the Si layer (Structure B and C) acts as a concentrator and enhances the local field more than five times compared to simple solar cells (Structure A).

The shape and position of the backside aluminum nano stripe must have been designed to spread the centralized light as much as possible and trap horizontally at the bottom of the cell. Nano stripes are placed in the lower part of the cell, which can be seen in Figs. 1c and d. The junction of these nanostripes is precisely located where the light intensity is maximized due to the surface hemisphere structure. Therefore, the amount of light absorption increases as the length of the light path through the cell or absorbent material increases.

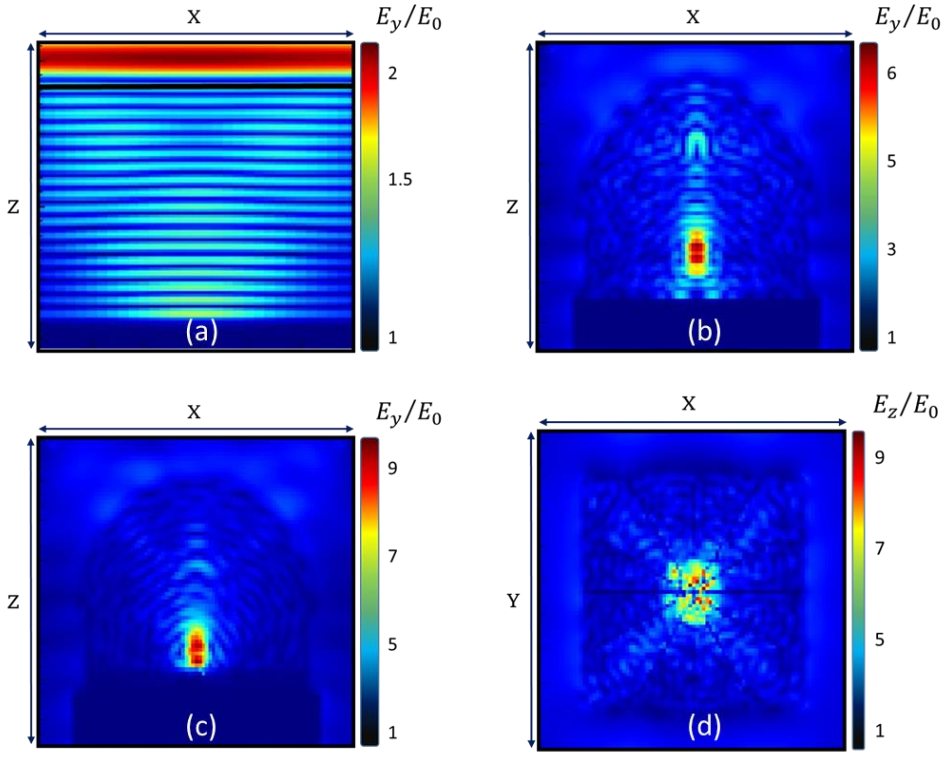

Fig.3. Electric field distribution of a) simple solar cell (structure A) in X-Z plane b) Si solar cell with hemisphere texturing on top (Structure B) in X-Z plane c) proposed Si solar cell with hemisphere texturing on top and metallic plasmonic nanostructure under the silicon layer Solar cell (Structure C) in X-Z plane d) proposed Si solar cell with hemisphere texturing on top and metallic plasmonic nanostructure under the silicon layer Solar cell (Structure C) in the X-Y plane.

The plasmonic property of metallic nanostructures can be analyzed using Maxwell equations. Since light is formed as electric and magnetic fields, when it collides with metal nanostructures, its fields cause nanostructures to act like a bipolar. In other words, it causes a displacement in metal surface electrons. Displacement of electrons causes localized fields and increases the electric field at the Si and Al interface and finally leads to high absorption [16]–[22]. Electric field distribution of the proposed structure at the surface of nanostripes is illustrated in Fig. 3d. As can be seen, the local field shows more than eight times enhancement compared to the simple solar cell. Moreover, the coupling of the electromagnetic waves and the nanograting structures can be predicted analytically. To do so, equations

$$K_{sp} = k_{in} sin\theta \pm m k_g \quad \text{and} \tag{9}$$

$$k_g = 2\pi / p \tag{10}$$

have to be satisfied for the sake of energy and momentum conservation between incident photons and surface plasmons[23], [24]. In these equations k_{sp} is the wave vector of surface plasmons at the interface of the metal/dielectric, θ is the angle between the normal vector of the grating plate and the incident light, m is an integer number indicating surface plasmon mode, k_g is the grating wave vector, and p is the periodicity of the grating. The value of k_{sp} in which ε_m is the relative permittivity of metal, and ε_d is the relative permittivity of dielectric is defined by ([23]–[26])

$$k_{sp} = \frac{2\pi}{\lambda}\sqrt{\frac{\varepsilon_d \varepsilon_m}{\varepsilon_d + \varepsilon_m}}. \tag{11}$$

For SPP mode, Eq. (9) and (10) are associated with the periodicity of the structure and Eq. (11) calculates the SPP wave vector. By substituting Eq. (6) and (7) in Eq. (5) and assuming$\theta = 0$, Eq. (11) will be reduced to

$$p = \alpha\lambda\left(\sqrt{\frac{\varepsilon_d \varepsilon_m}{\varepsilon_d + \varepsilon_m}}\right)^{-1}. \quad (12)$$

Due to the periodicity of the structure, there would be different order modes and α as the mode's order is defined as 1,2,3, etc.[23], [24].

The changes in the electric field at the nano strip surface cause a group movement of the electrons, which changes at a certain frequency. Now, if this frequency intensifies with the frequency of the light collision, the light moves at the common surface between metal and semiconductor, which named surface plasmon polariton. Polariton plasmons increase the length of the light pathway within the absorbent material, thereby increasing the absorption of the light [6], [10], [14], [27]–[31]. To illustrate the effect of the surface formation and addition of the metallic nanostripes from structure A to C simultaneously, figure 3 shows the light absorption efficiency in these three different structures. According to this figure, it can be seen that the simultaneous use of both approaches (surface forming and adding metal nanostructures to the solar cell) yields a better result. In the wavelengths ranging between 400 to 700 nm, as the main range for the sunlight, light absorption is approximately 40% higher compared to the previously published data provided in [17], [32].

Open circuit voltage, short circuit current density and fill factor of simple Si solar cell (Structure A), Si solar cell with hemisphere texturing on top (Structure B) and proposed Si solar cell with hemisphere texturing on top and metallic plasmonic nanostructure under the silicon layer (Structure c) are shown in Fig. 5a-c, respectively. As can be seen, the proposed structure results in 545 mV open-circuit voltage, 27.5 mA/cm^2 short circuit and 75% fill factor (FF). The short circuit current of the proposed structure is 65% higher than the simple Si solar cell. In order to explain the short circuit current enhancement, the generation rate has to be described in detail. The time-dependent carrier generation rate (G) has been calculated as

$$G(x,y,z,t) = (4\pi k_{PC}/hc)P_s(x,y,z)\exp\left(4\ln(0.5)\frac{(t-t_o)^2}{D_t^2}\right) \quad (13)$$

where k_{PC} represents the imaginary part of the refractive index, c is the speed of light, D_t is laser pulse duration, h is Planck's constant and $P_s(x,y,z)$ is total power flux density that can be obtained by Maxwell's equation solving. As can be interpreted from Eq. 13, by increasing the optical power inside the Si layer, the generation rate will increase. So, the number of excited electron-hole pairs will increase, and so the short current density.

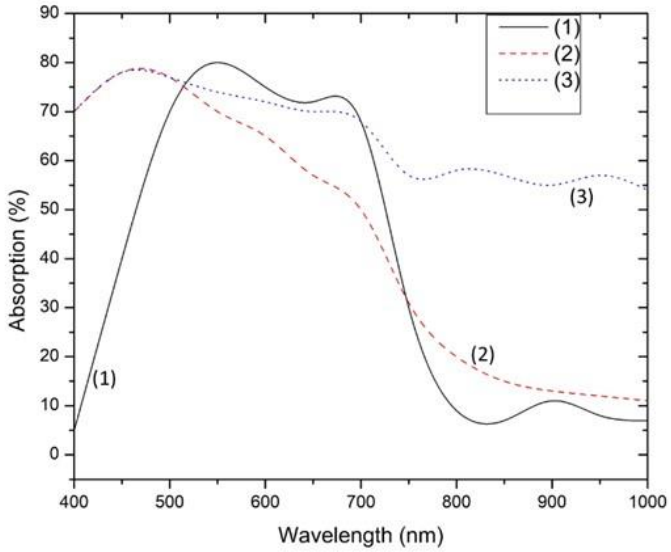

Fig. 4. Light absorption in three mentioned structures 1) flat cell surface without nano stripe 2) hemisphere textured cell without nano stripe 3) a textured cell with a hemisphere and with the addition of Aluminum nano stripe.

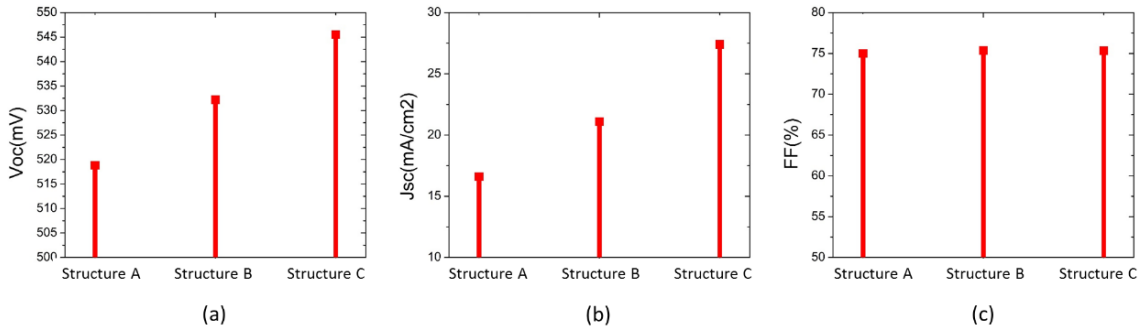

Fig. 5. a) Open circuit voltage b) short circuit current density and c) fill factor of the simple solar cell (structure A), Si solar cell with hemisphere texturing on top (Structure B) and proposed Si solar cell with hemisphere texturing on top and metallic plasmonic nanostructure under the silicon layer Solar cell

7. Conclusions

In summary, a Si solar cell with hemisphere texturing on top and metallic plasmonic nanostructure under the silicon layer is proposed, and using the FDTD method, the interaction of light with the proposed structure is investigated thoroughly. According to the results, the proposed structure shows more than 40% and 34% enhancement in average light absorption and solar cell efficiency, respectively. Moreover, the E-field distributions and short circuit current density of three different structures were investigated, and results demonstrate more than eight times enhancement for local electric field and 1.65 time enhancement for short circuit current density compared to the simple solar cell. This large short current density enhancement illustrates the potential of the proposed structure for improving the conversion efficiency of thin-film silicon solar cells.

References

[1] A. J. McEvoy, T. Markvart, L. Castañer, and L. Castaner, Practical Handbook of Photovoltaics: Fundamentals and Applications. Academic Press, 2012.

[2] A. Behzadi, E. Gholamian, E. Houshfar, M. Ashjaee, and A. Habibollahzade, "Thermoeconomic analysis of a hybrid PVT solar system integrated with double effect absorption chiller for cooling/hydrogen production," Energy Equip. Syst., vol. 6, no. 4, pp. 413–425, 2018.

[3] M. Bayareh, "Numerical simulation of a solar chimney power plant in the southern region of Iran," Energy Equip. Syst., vol. 5, no. 4, pp. 431–437, 2017.

[4] M. A. Green, "Lambertian Light Trapping in Textured Solar Cells and Light-Emitting Diodes: Analytical Solutions," vol. 241, no. May 2001, pp. 235–241, 2002.

[5] J. Poursafar, M. Kolahdouz, E. Asl Soleimani, and S. Golmohammadi, "Ultra-thin tandem-plasmonic photovoltaic structures for synergistically enhanced light absorption," RSC Adv., p. , 2016.

[6] S. Ghorbani, M. Bashirpour, J. Poursafar, M. Kolahdouz, M. Neshat, and A. Valinejad, "Thin-Film Tandem Nanoplasmonic Photoconductive Antenna for High-Performance Terahertz Detection," Superlattices Microstruct., 2018.

[7] J. Poursafar, M. Bashirpour, M. Kolahdouz, A. V. Takaloo, M. Masnadi-Shirazi, and E. Asl-Soleimani, "Ultrathin solar cells with Ag meta-material nanostructure for light absorption enhancement," Sol. Energy, vol. 166, pp. 98–102, 2018.

[8] P. H. Wang, M. Theuring, M. Vehse, V. Steenhoff, C. Agert, and A. G. Brolo, "Light trapping in a-Si: H thin-film solar

cells using silver nanostructures," AIP Adv., vol. 7, no. 1, p. 15019, 2017.

[9] H. A. Atwater and A. Polman, "Plasmonics for improved photovoltaic devices," Nat. Mater., vol. 9, no. 3, p. 205, 2010.

[10] D. M. Schaadt, B. Feng, and E. T. Yu, "Enhanced semiconductor optical absorption via surface plasmon excitation in metal nanoparticles," Appl. Phys. Lett., vol. 86, no. 6, p. 63106, 2005.

[11] S. Pillai, K. R. Catchpole, T. Trupke, and M. A. Green, "Surface plasmon enhanced silicon solar cells," J. Appl. Phys., vol. 101, no. 9, p. 93105, 2007.

[12] M. Bashirpour, A. Kefayati, M. Kolahdouz, and H. Aghababa, "Tuning the Electronic Properties of Symmetrical and Asymmetrical Boron Nitride Passivated Graphene Nanoribbons: Density Function Theory," in Journal of Nano Research, 2018, vol. 54, pp. 35–41.

[13] M. Bashirpour, S. Ghorbani, M. Kolahdouz, M. Neshat, M. Masnadi-Shirazi, and H. Aghababa, "Significant performance improvement of a terahertz photoconductive antenna using a hybrid structure," RSC Adv., vol. 7, no. 83, pp. 53010–53017, 2017.

[14] M. Bashirpour, M. Kolahdouz, and M. Neshat, "Enhancement of optical absorption in LT-GaAs by double-layer nanoplasmonic array in photoconductive antenna," Vacuum, vol. 146, pp. 430–436, 2017.

[15] M. Gharghi, "Spherical Silicon for Photovoltaic Application: Material, Modeling, and Devices," UWSpace, 2008.

[16] K. R. Catchpole and A. Polman, "Design principles for particle plasmon enhanced solar cells," Appl. Phys. Lett., vol. 93, no. 19, p. 191113, 2008.

[17] J.-D. Hwang and D.-R. Hsieh, "A surface-plasmon-enhanced silicon solar cell with KOH-etched pyramid structure," IEEE Electron Device Lett., vol. 34, no. 5, pp. 659–661, 2013.

[18] N. Zhou, V. López-Puente, Q. Wang, L. Polavarapu, I. Pastoriza-Santos, and Q.-H. Xu, "Plasmon-enhanced light-harvesting: applications in enhanced photocatalysis, photodynamic therapy and photovoltaics," Rsc Adv., vol. 5, no. 37, pp. 29076–29097, 2015.

[19] F. Taghian, V. Ahmadi, and L. Yousefi, "Enhanced thin solar cells using optical nano-antenna induced hybrid plasmonic traveling-wave," J. Light. Technol., vol. 34, no. 4, pp. 1267–1273, 2016.

[20] V. E. Ferry, M. A. Verschuuren, H. B. T. Li, E. Verhagen, R. J. Walters, R. E. I. Schropp, H. A. Atwater, and A. Polman, "Light trapping in ultrathin plasmonic solar cells," Opt. Express, vol. 18, no. 102, pp. A237--A245, 2010.

[21] R. B. Dunbar, T. Pfadler, and L. Schmidt-Mende, "Highly absorbing solar cells—a survey of plasmonic nanostructures," Opt. Express, vol. 20, no. 102, pp. A177--A189, 2012.

[22] R. A. Pala, J. White, E. Barnard, J. Liu, and M. L. Brongersma, "Design of Plasmonic Thin-Film Solar Cells with Broadband Absorption Enhancements," Adv. Mater., vol. 21, no. 34, pp. 3504–3509, 2009.

[23] P. Karpinski and A. Miniewicz, "Surface Plasmon Polariton Excitation in Metallic Layer Via Surface Relief Gratings in Photoactive Polymer Studied by the Finite-Difference Time-Domain Method," Plasmonics, vol. 6, no. 3, pp. 541–546, 2011.

[24] S. A. Maier, Plasmonics - Fundamentals and Applications. Springer, 2007.

[25] R. Wang, T. Li, X. Shao, X. Li, and H. Gong, "The simulation of localized surface plasmon and surface plasmon polariton in wire grid polarizer integrated on InP substrate for InGaAs sensor," AIP Adv., vol. 5, no. 7, pp. 1–6, 2015.

[26] N. M. Burford, M. J. Evans, and M. O. El-Shenawee, "Plasmonic Nanodisk Thin-Film Terahertz Photoconductive Antenna," IEEE Trans. Terahertz Sci. Technol., vol. 8, no. 2, pp. 237–247, 2018.

[27] V. E. Ferry, J. N. Munday, and H. A. Atwater, "Design considerations for plasmonic photovoltaics," Adv. Mater., vol. 22, no. 43, pp. 4794–4808, 2010.

[28] R. Biswas and D. Zhou, "Simulation and modeling of photonic and plasmonic crystal back reflectors for efficient light trapping," Phys. status solidi, vol. 207, no. 3, pp. 667–670, 2010.

[29] C. Tang, Z. Yan, Q. Wang, J. Chen, M. Zhu, B. Liu, F. Liu, and C. Sui, "Ultrathin amorphous silicon thin-film solar cells by magnetic plasmonic metamaterial absorbers," RSC Adv., vol. 5, no. 100, pp. 81866–81874, 2015.

[30] S. Ghorbani, M. Bashirpour, M. Forouzmehr, M. R. Kolahdouz, and M. Neshat, "Simulation of THz photoconductive antennas loaded by different metallic nanoparticles," in 2016 Fourth International Conference on Millimeter-Wave and Terahertz Technologies (MMWaTT), 2016, pp. 62–64.

[31] S. Ghorbani, M. Bashirpour, M. Kolahdouz, M. Neshat, M. Mansouree, and M. Forouzmehr, "Improving Efficiency of THz Photoconductive Antennas Using Nano Plasmonic Structure," in Asia Communications and Photonics Conference 2016, 2016, p. AF2A.73.

[32] G. Sun, T. Gao, X. Zhao, and H. Zhang, "Fabrication of micro/nano dual-scale structures by improved deep reactive ion etching," J. Micromechanics Microengineering, vol. 20, no. 7, p. 75028, 2010.